

Hydrocarbon Potential of Nigeria's Inland Basin: Case Study of Afikpo Basin

¹ Ibe Stephen O., ² Uche Iduma

¹ Federal University Otuoke Bayelsa, Nigeria, ² Nigerian Geological Survey Agency, Abuja
Corresponding Author: Ibe Stephen O.

Abstract; *The thermo-tectonic event during the Santonian created the Afikpo Basin. Afikpo Basin is filled with Cretaceous sediments aged Albian to Maastrichtian. This work interprets aeromagnetic data over the basin to define the structural complexity, depth to basement and sedimentary thickness within the Basin, which would serve as an aid to further exploratory work in the basin. Analytic signal, first vertical derivative and source parameter imaging were applied to enhance the data for interpretation. The structures within the basin trend majorly in the NE-SW direction with minor NW-SE and NS trends. Lineament density analysis showed that sediments at the east of Afikpo, east of Biakpan, Itu, Uyo, Nto Ndan, Abekenta, Uturu, Otampa, Ovim, Owutu, Ngusu, Ishiagu and Mpu underwent intense deformation. Sediments of Amasiri, Akaeze, Abiriba, Ohafia, Uduk Usung, Abak and Odoro Ikpe underwent moderate deformation while Arochukwu, Uburu, Amaeke, Amawon and Oko Ita sediments experience the least level of deformation. Source parameter imaging estimated average sediment thicknesses at Ndiobasi, Ohafia, Biakpan, Otampa, Amaeke, Arochukwu, Uyo, Uduk Usung and Ikot Ekpene to be 4.5 km, 2.6 km, 2.1 km, 2.0 km, 3.9 km, 3.0 km, 1.5 km, 2.6 km and 4.2 km respectively. Ndiobasi, Ohafia, Biakpan, Amaeke, Arochukwu, Uduk Usung and Ikot Ekpene were defined to have great potentials for generating and accumulating hydrocarbon, if other conditions necessary for its generation are present. These areas were recommended for further studies on the bases of their sediment structural complexities and sediment thicknesses.*

Keywords: *Hydrocarbon, Inland Basin, Afikpo, Arochukwu, Ikot Ekpene, aeromagnetic, first vertical derivative, analytic signal, source parameter imaging, exploration, sediment thickness.*

I. Introduction

The Benue Trough was installed as pull-apart sub-basins generated by sinistral strike-slip displacements inherited from pre-existing transcurrent fault zones in the Pan African mobile belt (Benkhelil, 1989; Nwajide, 2013). It is part of the much larger West and Central African Rift System (Fairhead, 1988; Genik, 1993) which originated during the breakup of the Gondwana supercontinent and the opening up of the southern Atlantic and Indian Oceans in the Jurassic (Burke et al., 1972; Benkhelil, 1982, 1989; Fairhead, 1988). Murat (1972) suggests that the southern portion of the Benue Trough was longitudinally faulted with its eastern half subsiding preferentially to become the Abakaliki depression. The thermo-tectonic event during the Santonian created the Afikpo Basin (east) and Anambra Basin (west) of the Anticlinorium.

The Afikpo Sub-basin was installed alongside the Anambra Basin as flexural basins, relative to the Abakaliki Anticlinorium after the Santonian Orogeny. The Afikpo Sub-basin (Figure 1) often referred to as the Afikpo syncline rests unconformably on the folded Pre-Santonian Abakaliki Anticlinorium, filled with Pre-Santonian sediments of the Asu-River Group and the Eze-aku Group (Murat, 1972). The syncline is a narrow asymmetrical depression, gently plunging southwards; it is aerially flanked in the northeast and northwest by the Abakaliki Fold Belt, in the east by the Calabar Flank and in the south by the Niger Delta. Reymont (1965) and Murat (1972) described the Afikpo Syncline and Anambra Basin and noted that sedimentation was controlled dominantly by transgression and regressions that led to deposition in a wide variety of environments ranging from fluvial through fluvio-marine environments.

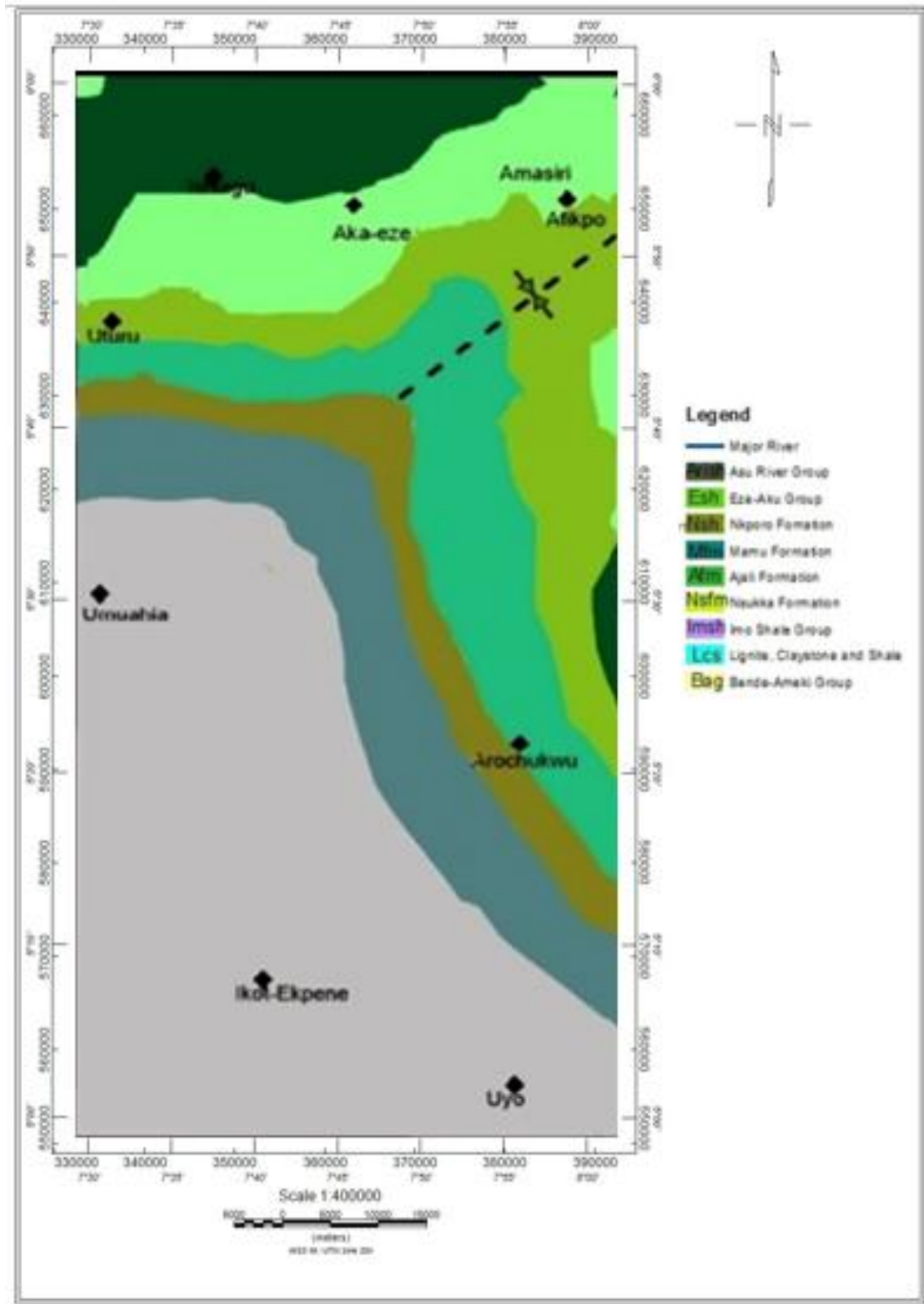


Figure 1: Geology of the Study Area

Sedimentation in the southern Benue Trough began with initial deposition of alluvial fans and lacustrine deposits during the Aptian – Albian period (Murat, 1972 and Hoque, 1977). The sediments belong to the Mamfe Formation (Reyment, 1965) and Ogoja Formation (Uzuakpunwa, 1974) of the Asu River Group. Three phases of marine transgression and regression occurred within the Albian to the Coniacian (Nwajide, 2013) and gave rise to mudrock, sandstone, limestone deposits and pyroclastic flows with an estimated thickness

of 3,500 m (Murat, 1972; Hoque, 1977). These deposits have been described as the Asu River Group (Aptian - Albian), the Odukpani Group (late Albian - Cenomanian), the Eze Aku Group (late Cenomanian – late Turonian) and the Awgu Shale (latest Turonian - Coniacian). Afikpo Sub-basin is filled by a thick sedimentary sequence of Campanian-Maastrichian deposits of shale, sandstone, siltstone, mudstone and coal. The Nkporo Formation (Simpson, 1954; Reyment, 1965) is the basal unit of the Afikpo sub-basin. The two basins (Anambra and Afikpo) are not contiguous having been separated by the Hawal-Kaltungo-Gboko-Abakaliki Anticlinorial ridge. Each basin had its delimiting basinal boundaries (Benkhelil *et al.*, 1989) and could not be the same as suggested by Nwajide (2006).

Previous geophysical work done within the study area (Onuba *et al.*, 2013; Onwuemesi 1995; Onwuemesi 1997; Ugbor and Okeke 2010; Ugwu *et al.* 2013; Ugwu and Ezema 2012; Anyanwu and Mamah 2013) dwelt more on the basin's origin, sediment thickness and petroleum potentials using forward and inverse modelling technique and spectral analysis but these methods have limitations (Petre and Randolph 2015). This work used the recent high resolution aeromagnetic data acquired by Fugro Airborne Survey over Nigeria with the aim to evaluate the structural complexity and sediment thickness.

1.1 The Study Area

The area is bounded by longitudes 7°30' 00"E to 8°30' 00"E and latitudes 5°30' 00"N to 6°30' 00"N. The study area covers approximately 6,050 km²; it is bounded by Onicha and Nenwe to the north, Ikot Etim and Ikot Eba to the south, Ndealiche and Ugep to the east and Okigwe and Owerrinta to the west. The area can be accessed through Abakaliki Afikpo expressway, Umuahia Afikpo expressway and Ikot Ekpene Afikpo expressway. It falls within the humid tropical region with two distinct seasons, the rainy season, from March to October, and dry season, from November to March.

II. Materials and Method

2.1 Data Acquisition

The aeromagnetic dataset used for this study is from the high-resolution airborne survey coverage in Nigeria carried out by Fugro Airborne Survey at 826,000 along a series of NW – SE flight lines of magnetic and radiometric surveys flown at 500 m line spacing and 80 m terrain clearance in 2009 and was obtained from the Nigerian Geological Survey Agency. The parameter measured was the total magnetic field. It consists of two square blocks of map sheets (313, 322) of square block which represents a map on the scale of 1:400,000 and is (55x110) km² covering an area of 6,050 km². The total magnetic intensity grid was generated using a minimum curvature algorithm at a grid cell size of 1,000 m. The digitized data were filtered using a low pass Fourier domain sub-routine filter to eliminate unwanted wavelengths and to pass longer wavelengths. Reduction-to-pole (RTP) transformation was applied to the aeromagnetic data to minimize polarity effects. These effects are manifested as a shift of the main anomaly from the center of the magnetic source and are due to the vector nature of the measured magnetic field. The RTP transformation usually involves an assumption that the total magnetizations of most rocks align parallel or anti-parallel to the Earth's main field.

2.2 Data Processing and Enhancement

2.2.1 Regional - residual Separation

Separation of regional and residual anomaly was done using Trend analysis in which a linear trend surface was fitted into the total aeromagnetic field data by a multiple regression technique for the purpose of removing the regional magnetic field. The linear surface fitted was removed from the regional component to obtain the residual magnetic anomaly map that was interpreted.

$$\text{Total field} = \text{Regional field} + \text{Residual field} \tag{1}$$

$$\text{Residual field} = \text{Total field} - \text{fitted Surface/Regional} \tag{2}$$

The Regional Field can be represented using the trend surface equation. Davis, (1973) expressed the regional field as;

$$\text{Regional Field} = a + bx_i + cy_j \tag{3}$$

Where, a, b and c are constants, x_i and y_j are coordinates in x and y directions.

Let Z_{ij} = the observed Total Field at ij^{th} data point.

Therefore,

$$\text{Total Field} (Z_{ij}) = (a + bx_i + cy_j) + \text{Residual Field} \tag{4}$$

Hence,

$$\text{Residual Field} = Z_{ij} - (a + bx_i + cy_j) \tag{5}$$

For a given magnetic data, the best fitting surface has the least square error,

$$\text{fitting error} = t - a - bx - cy \tag{6}$$

Where t is the magnetic value at x and y coordinate point.

Note that a, b and c are unknown coefficients while t, x and y are given. To obtain the least square error, the unknown coefficients a, b and c must yield zero first partial derivative.

Hence, the sum of the square of the fitting error becomes;

$$\sum_{i=1}^N \sum_{j=1}^N (\text{fitting error})^2 = \sum_{i=1}^N \sum_{j=1}^N (t_{ij} - a - bx_i - cy_j)^2 \tag{7}$$

where x_i, y_j and t_{ij} are vectors and i and j are unit vector while t, x and y are coefficient of the unit vector.

$$M = \sum_{i=1}^N \sum_{j=1}^N (t_{ij} - a - bx_i - cy_j)^2 \tag{8}$$

Taking the partial derivative of equation (8) with respect to a and equate it to zero,

$$\sum_{i=1}^N \sum_{j=1}^N t_{ij} - \sum_{i=1}^N \sum_{j=1}^N a - b \sum_{i=1}^N \sum_{j=1}^N x_i - c \sum_{i=1}^N \sum_{j=1}^N y_j = 0 \tag{9}$$

Partial derivative of the second constant b and equating it to zero;

$$\sum_{i=1}^N \sum_{j=1}^N t_{ij} x_i - a \sum_{i=1}^N \sum_{j=1}^N x_i - b \sum_{i=1}^N \sum_{j=1}^N x_i^2 - c \sum_{i=1}^N \sum_{j=1}^N x_i y_j = 0 \tag{10}$$

Taking the partial derivative of the third constant c;

$$\sum_{i=1}^N \sum_{j=1}^N t_{ij} y_j - a \sum_{i=1}^N \sum_{j=1}^N y_j - b \sum_{i=1}^N \sum_{j=1}^N x_i y_j - c \sum_{i=1}^N \sum_{j=1}^N y_j^2 = 0 \tag{11}$$

Solving this series of simultaneous equations will give the coefficients of the best fitting linear trend surface, being defined by the least-square criterion. The above equation can be written into matrix form as:

$$\begin{bmatrix} N & \sum_{i=1}^N \sum_{j=1}^N x_i & \sum_{i=1}^N \sum_{j=1}^N y_j \\ \sum_{i=1}^N \sum_{j=1}^N x_i & \sum_{i=1}^N \sum_{j=1}^N x_i^2 & \sum_{i=1}^N \sum_{j=1}^N x_i y_j \\ \sum_{i=1}^N \sum_{j=1}^N y_j & \sum_{i=1}^N \sum_{j=1}^N x_i y_j & \sum_{i=1}^N \sum_{j=1}^N y_j^2 \end{bmatrix} \begin{bmatrix} a \\ b \\ c \end{bmatrix} = \begin{bmatrix} \sum_{i=1}^N \sum_{j=1}^N t_{ij} \\ \sum_{i=1}^N \sum_{j=1}^N t_{ij} x_i \\ \sum_{i=1}^N \sum_{j=1}^N t_{ij} y_j \end{bmatrix} \tag{12}$$

The values of a, b, and c were obtained as follows;

$$\left. \begin{array}{l} a = 7923 \\ b = 3.4261 \\ c = -3.6231 \end{array} \right\} \tag{13}$$

The trend surface equation (regional gradient) becomes:

$$T(x, y) = 7923 + 3.4261x - 3.6231 y \tag{14}$$

Furthermore, the trend surface equation was then subtracted from the aeromagnetic (observed) data and the resultant residual anomaly was digitized.

2.2.2 Analytic Signal Filter

Nabighian (1972) suggested the concept of analytic signal (AS) and proposed that in the 2-D case, the horizontal and vertical derivatives of magnetic fields satisfy the Hilbert transform, thus can be regarded as analytic signals. The amplitude of the analytic signal is the same as the total gradient, independent of the direction of magnetization, and represents the envelope of both the vertical and horizontal derivatives over all possible directions of the earth's field and source magnetization (Luo *et al.*, 2011).

$$\frac{\partial T}{\partial z} = H \left[\frac{\partial T}{\partial x} \right] \tag{15}$$

Where;

T = Magnetic anomaly data

H = Hilbert transform

The analytical signal of a real signal f is defined as;

$$AS \left(\frac{\partial T}{\partial x} \right) = \frac{\partial T}{\partial x} - iH \left[\frac{\partial T}{\partial x} \right] \tag{16}$$

Where:

$$i = -1 \text{ (Luo et al., 2011)}$$

According to the definition, the analytical signal of the potential field obtained by combining this two quantities into a two-dimensional quantity known as the analytic signal is given as;

$$AS(x, z) = \frac{\partial T}{\partial x} + i \frac{\partial T}{\partial z} \tag{17}$$

Where:

$$\frac{\partial T}{\partial x} \text{ and } \frac{\partial T}{\partial z} = \text{Horizontal and vertical component of the total field respectively,}$$

$T(x, z)$ = Magnitude of the total magnetic field

z and x = Cartesian coordinates for the vertical direction and the direction perpendicular to strike respectively

The amplitude of the analytic signal is defined as;

$$|AS(z)| = \sqrt{\left(\frac{\partial T}{\partial x}\right)^2 + \left(\frac{\partial T}{\partial z}\right)^2} \quad (18)$$

The amplitude of the analytic signal is a symmetric bell-shaped function. By examining its profile across a magnetic source, the analytic signal can be used in interpretation to provide an indication of the edges of the causative body. Similarly for the three dimensional case, the analytic signal is given by;

$$AS(x, y) = \left(\frac{\partial T}{\partial x}\right) + \left(\frac{\partial T}{\partial y}\right) + \left(i \frac{\partial T}{\partial z}\right) \quad (19)$$

Where its amplitude is defined as;

$$|AS(x, y)| = \sqrt{\left(\frac{\partial T}{\partial x}\right)^2 + \left(\frac{\partial T}{\partial y}\right)^2 + \left(\frac{\partial T}{\partial z}\right)^2} \quad (20)$$

The maximum value of the analytic signal determines the edges of a magnetic body.

2.2.3 First Vertical Derivative

Derivatives (vertical) are based on the principle that the rates of change of magnetic field are sensitive to rock susceptibilities near the ground surface than at depth. First vertical derivative is physically equivalent to measuring the magnetic field simultaneously at two points vertically above each other, subtracting the data and dividing the result by the vertical spatial separation of the measurement points. The first vertical derivative was obtained from Laplace equation which is used to describe the magnetic potential field (U) thus,

$$\frac{\partial^2 U}{\partial x^2} + \frac{\partial^2 U}{\partial y^2} + \frac{\partial^2 U}{\partial z^2} = 0 \quad (21)$$

$$\text{but, } -\text{grad } U = T \quad (22)$$

Hence,

$$-\frac{\partial T}{\partial x} - \frac{\partial T}{\partial y} - \frac{\partial T}{\partial z} = 0 \quad (23)$$

Therefore,

$$\frac{\partial T}{\partial z} = -\left(\frac{\partial T}{\partial x} + \frac{\partial T}{\partial y}\right) \quad (24)$$

Where, $U = \text{magnetic potential field}$

$T = \text{total magnetic field vector}$

Rewriting equation (24) in numerical form we have,

$$-\frac{\partial T}{\partial x} = \left[\frac{T(x+\Delta x) - T(x)}{\Delta x} + 0(\Delta x)\right] \quad (25)$$

$$0(\Delta x) = \text{error terms} \quad (26)$$

$$-\frac{\partial T}{\partial x} = \left[\frac{T(x+\Delta x) - T(x)}{\Delta x}\right] \quad (27)$$

Similarly,

$$-\frac{\partial T}{\partial y} = \left[\frac{T(y+\Delta y) - T(y)}{\Delta y}\right] \quad (28)$$

Therefore,

$$\frac{\partial T}{\partial z} = -\left[\frac{T(x+\Delta x) - T(x)}{\Delta x}\right] - \left[\frac{T(y+\Delta y) - T(y)}{\Delta y}\right] \quad (29)$$

Equation (29) was applied on TMI grid to produce the first derivative map.

$\Delta x = \text{grid interval in } x - \text{direction}$

$\Delta y = \text{grid interval in } y - \text{direction}$

2.2.4 Source Parameter Imaging (SPI)

This technique was developed by Thurston and Smith (1997) and Thurston et al. (1999, 2002). The Source Parameter Imaging (SPI) has accuracy shown to be +/- 20% in tests on real data sets with drillhole control. It is a profile or grid-based method for estimating magnetic source depths, and for some source geometries the dip and susceptibility contrast. The method utilizes the relationship between source depth and the local wavenumber (k) of the observed field, which can be calculated for any point within a grid of data via horizontal and vertical gradients (Thurston and Smith, (1997) hence SPI method requires first- and second-order derivatives and is thus susceptible to both noise in the data and to interference effects. The SPI method (Thurston and Smith, 1997) estimates the depth from the local wave number of the analytical signal. Figure 2 is a right angle triangle obtained from Argand Diagram and used to simplify the following expression.

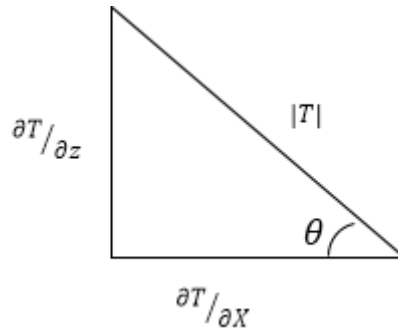


Figure 2: Right Angle Triangle Obtained from Argand Diagram

$$|T| = \sqrt{\left(\frac{\partial T}{\partial x}\right)^2 + \left(\frac{\partial T}{\partial z}\right)^2} \tag{30}$$

Where;

$|T|$ = The absolute magnetic wave amplitude θ is the phase spectrum or phase angle defines by;

$$\theta = \tan^{-1} \left(\frac{\frac{\partial T}{\partial z}}{\frac{\partial T}{\partial x}} \right) \tag{31}$$

In the analysis of potential fields, it is more convenient to use wavenumber, denoted by k . (Thurston and Smith, 1997), the wavenumber (k) concept I used to define the magnetic source.

$$k = \frac{\partial \theta}{\partial x} \tag{32}$$

Substituting equation (30) into (31) we have;

$$k = \frac{\partial}{\partial x} \tan^{-1} \left(\frac{\frac{\partial T}{\partial z}}{\frac{\partial T}{\partial x}} \right) \tag{33}$$

Differentiating equation (33), we have

$$k = \frac{1}{|T|^2} \times \left(\frac{\partial T}{\partial x} \frac{\partial^2 T}{\partial x \partial z} - \frac{\partial T}{\partial z} \frac{\partial^2 T}{\partial x^2} \right) \tag{34}$$

By considering a surface, the expression for the vertical and horizontal components of the magnetic signal are given by (Nabighian, 1972) as follows;

$$vertical = \frac{\partial T}{\partial z} = 2KFc \sin d \times \frac{x \cos (2I-d-90) - h \sin (2I-d-90)}{h^2+x^2} \tag{35}$$

$$horizontal = \frac{\partial T}{\partial x} = 2KFc \sin d \times \frac{h \cos (2I-d-90) + x \sin (2I-d-90)}{h^2+x^2} \tag{36}$$

Where

K = Susceptibility contrast

F = Magnitude of the ambient field

$c = 1 - \cos^2 I \sin^2 \alpha$ = Ambient field declination

I = Inclination of the ambient field

d = Angle of dip of the body and h is the depth to the top of the magnetic contact.

Substituting equation (34) and (35) into equation (36) and solving accordingly;

$$k = \frac{h}{h^2+x^2} \tag{37}$$

At directly over the edge of the magnetic source, $x = 0$, bearing in mind that the wavenumber is independent of the magnetization direction, i.e. at the maxima of the local wavenumber, the peaks of the magnetic anomaly outline the magnetic source edges at $x = 0$. (Thurston and Smith, 1997) defined the depth (h) at this point as;

$$h = \frac{1}{k} \tag{38}$$

III. Result and Discussion

3.1 Results

The total magnetic intensity map (Figure 3) reflects magnetic variation of both regional (deep sited bodies) and residual (shallow sited structures). Trend analysis filter is applied to the total magnetic intensity in

order to produce the residual magnetic anomaly map of the study area (Figure 4), which displays susceptibility variation locally and have exploration significance.

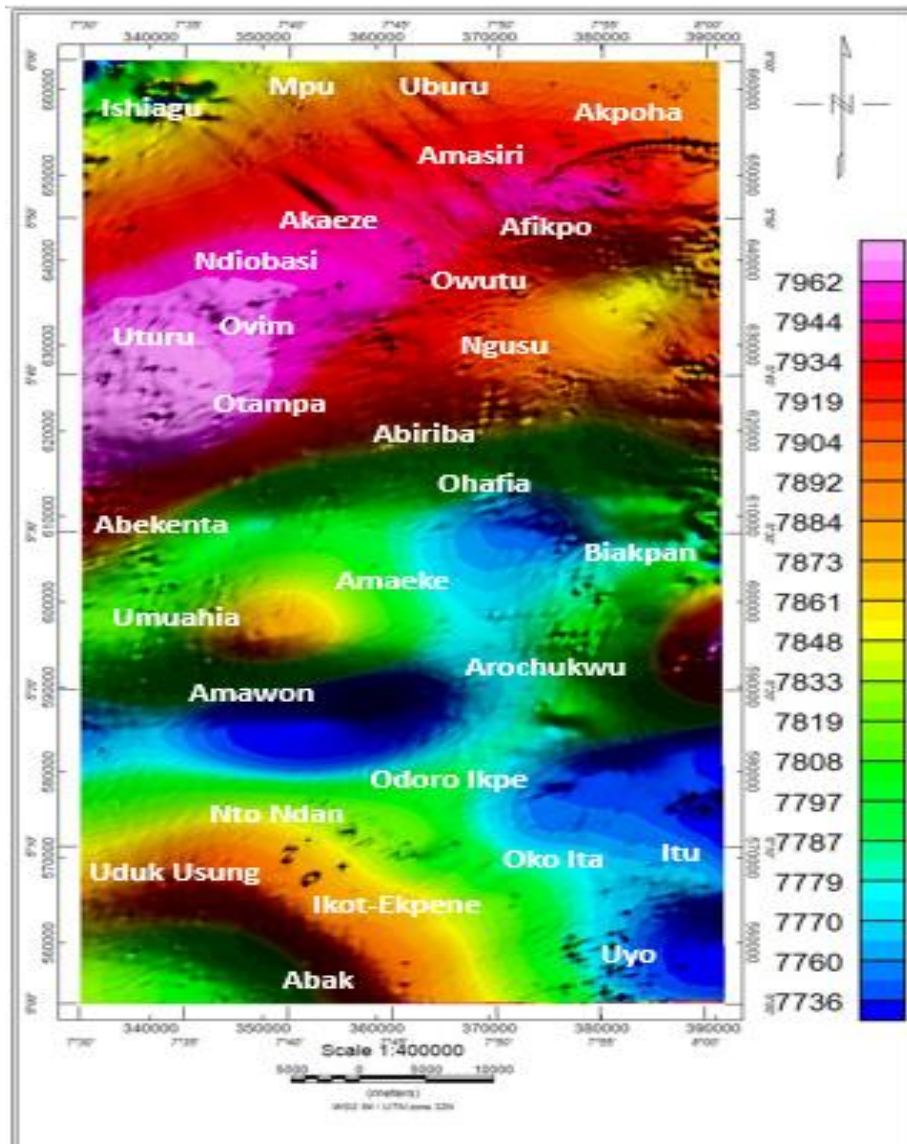


Figure 3: Total Magnetic Intensity (TMI) Map of the Study Area

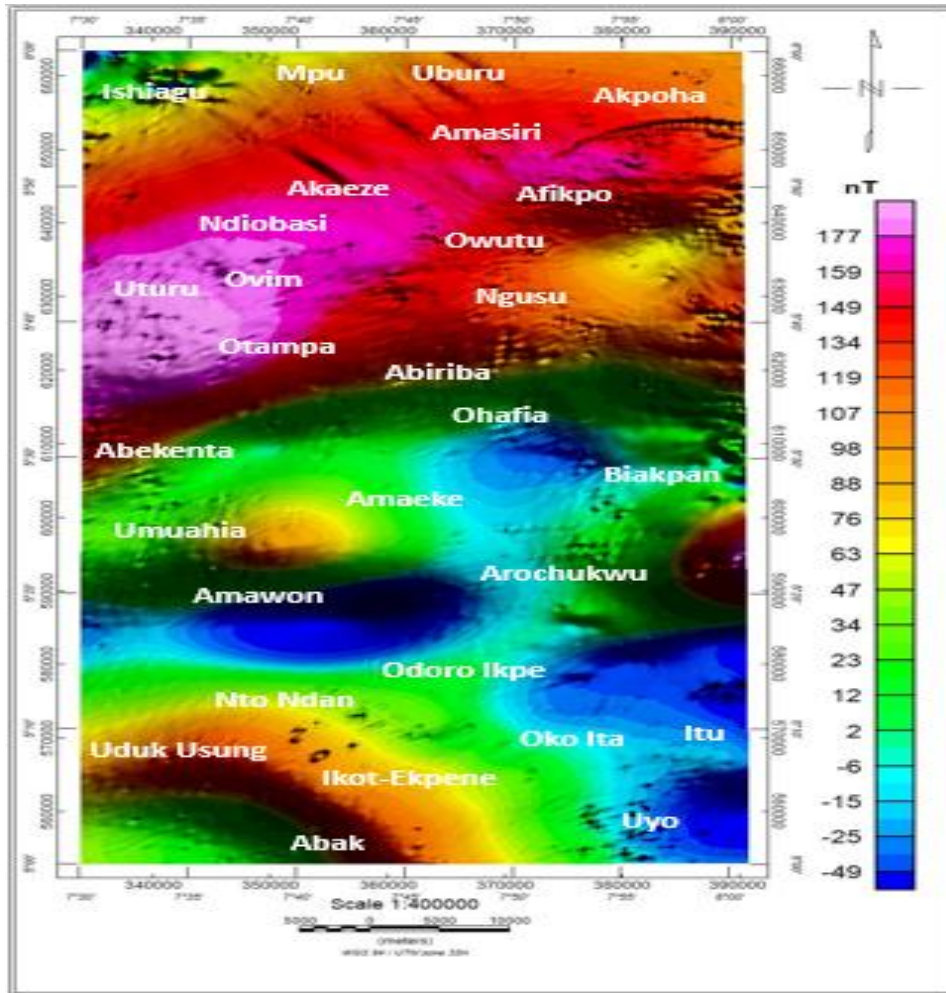


Figure 4: Residual Magnetic Intensity (RMI) Map of the Study Area

Analytic signal of the residual data was computed and plotted (Figure 5). This gives a very clean view of the magnetic anomalies (Ansari and Alamdar, 2011). The analytic signal filter was applied to the total magnetic intensity dataset to enhance the edge of the shallow magnetic source in order to identify structures and intruded zones within the study area.

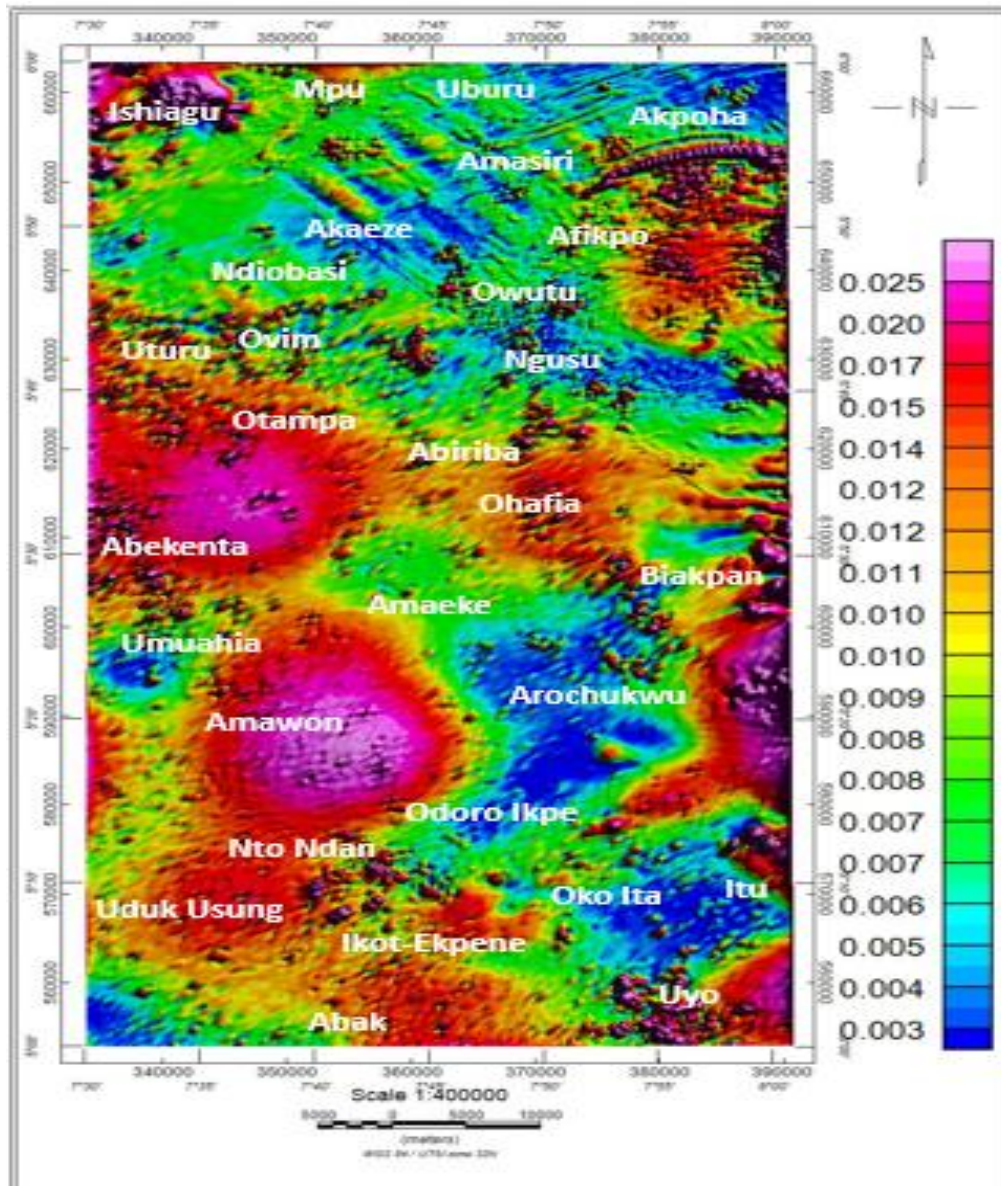


Figure 5: Analytic Signal Map of the Study Area

To amplify structures First Vertical Derivative (FVD) was computed (Figure 6) in order to enhance and sharpen up anomalies over causative bodies and tend to reduce complexity, allowing a clearer imaging of the causative structures. Lineament was extracted from the data (Figure 7) using center for exploration targeting (CET) grid analysis. CET enhances, locates and vectorises discontinuity structures within the potential field data (Siddorn and Hills, 2002). Lineaments are structural deformations that are related to faults, joints, and arched zones or even geological contacts. Magnetic minerals are mainly concentrated along or aligned with some structures or sedimentary features such as faults or channels. Rose diagram (Figure 7) was produced to determine the trend of structures in the study area.

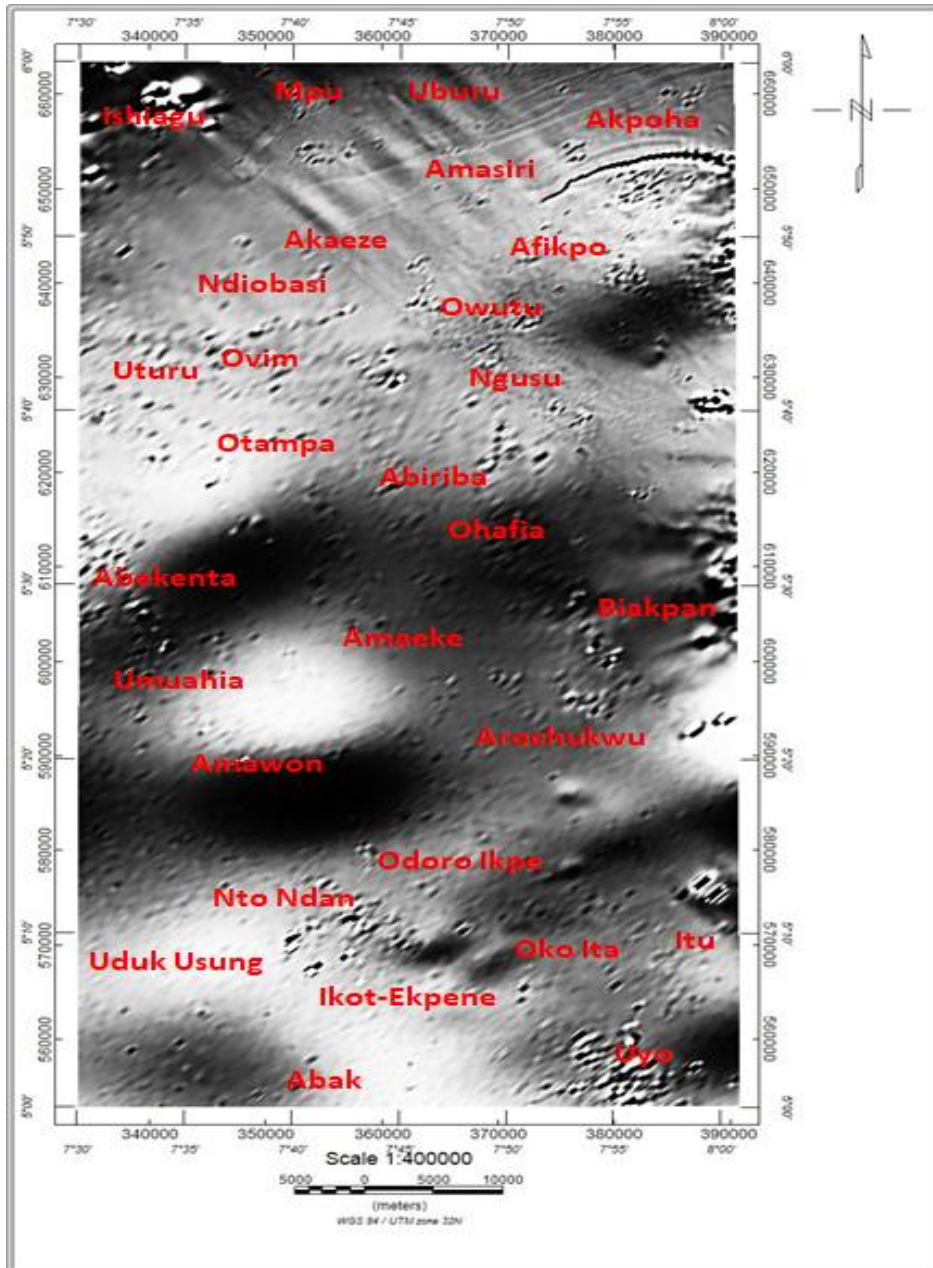


Figure 6: First Vertical Derivative (FVD) Map of the Study Area

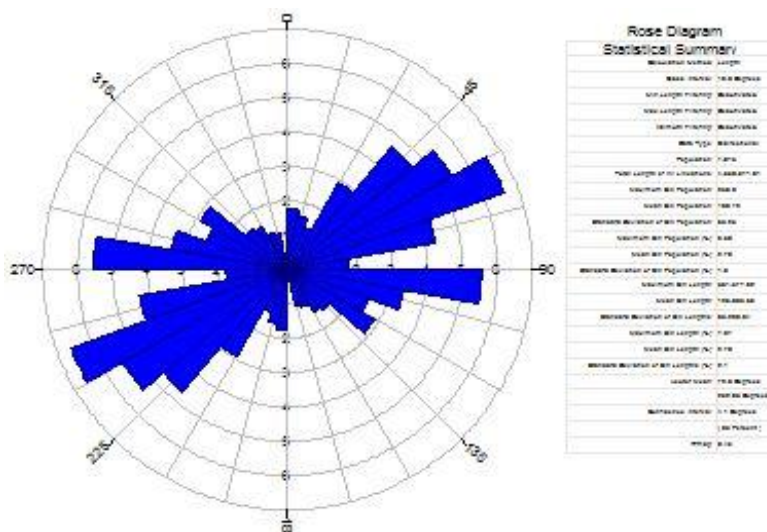
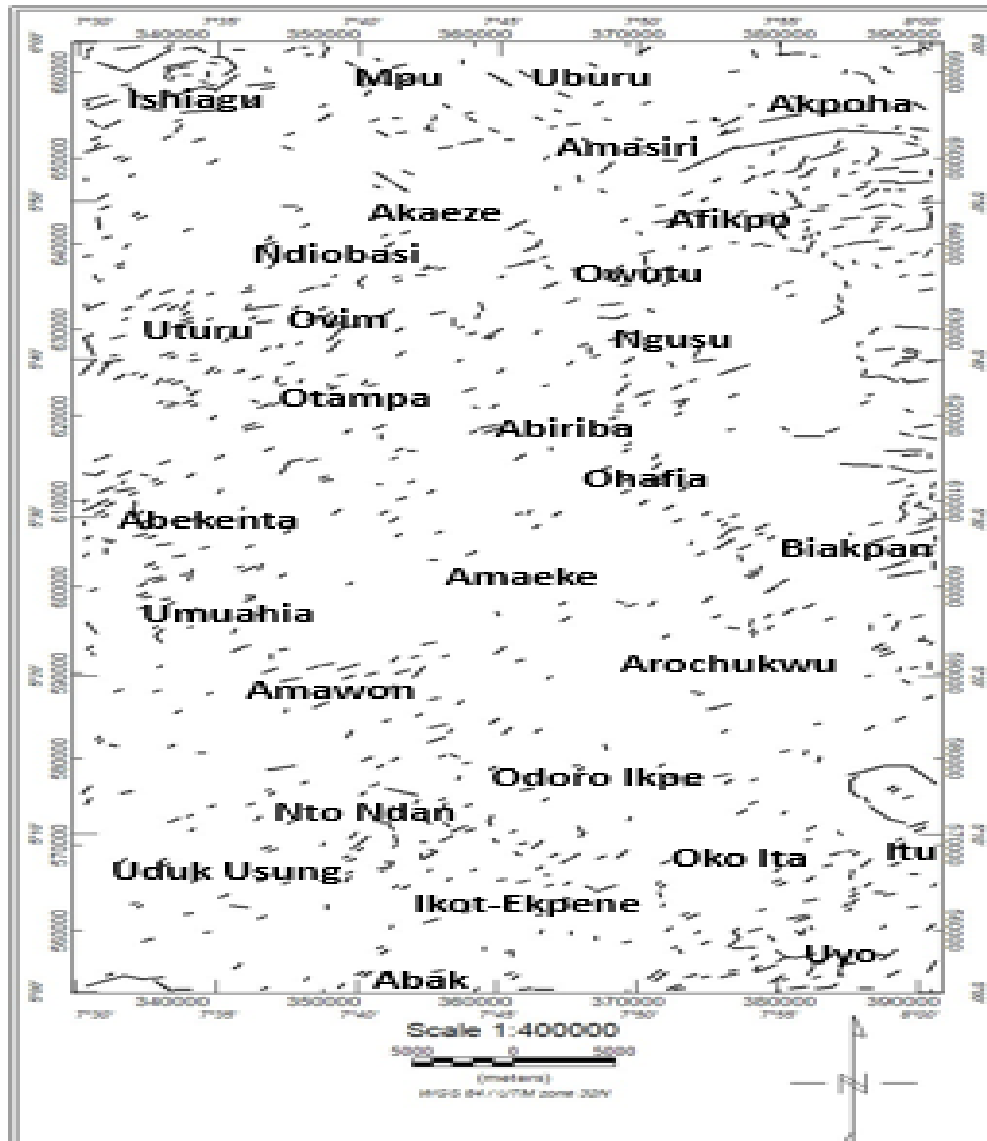


Figure 7: Lineament Map and Rose Diagram of the Study Area

Source Parameter Imaging (SPI) of the study area was computed and the corresponding SPI data was plotted to define a depth to magnetic basement within the study area. Source parameter imaging (SPI) was

adhered to, as the method is much more sensitive to noise at higher derivative order. Therefore, careful filtering of data was ensured so as to have good estimates of the local wave number and hence the depth. The source parameter imaging map (Figure 8) shows the depth estimate to the top of the sediment/basement interface (Smith et al, 1998).

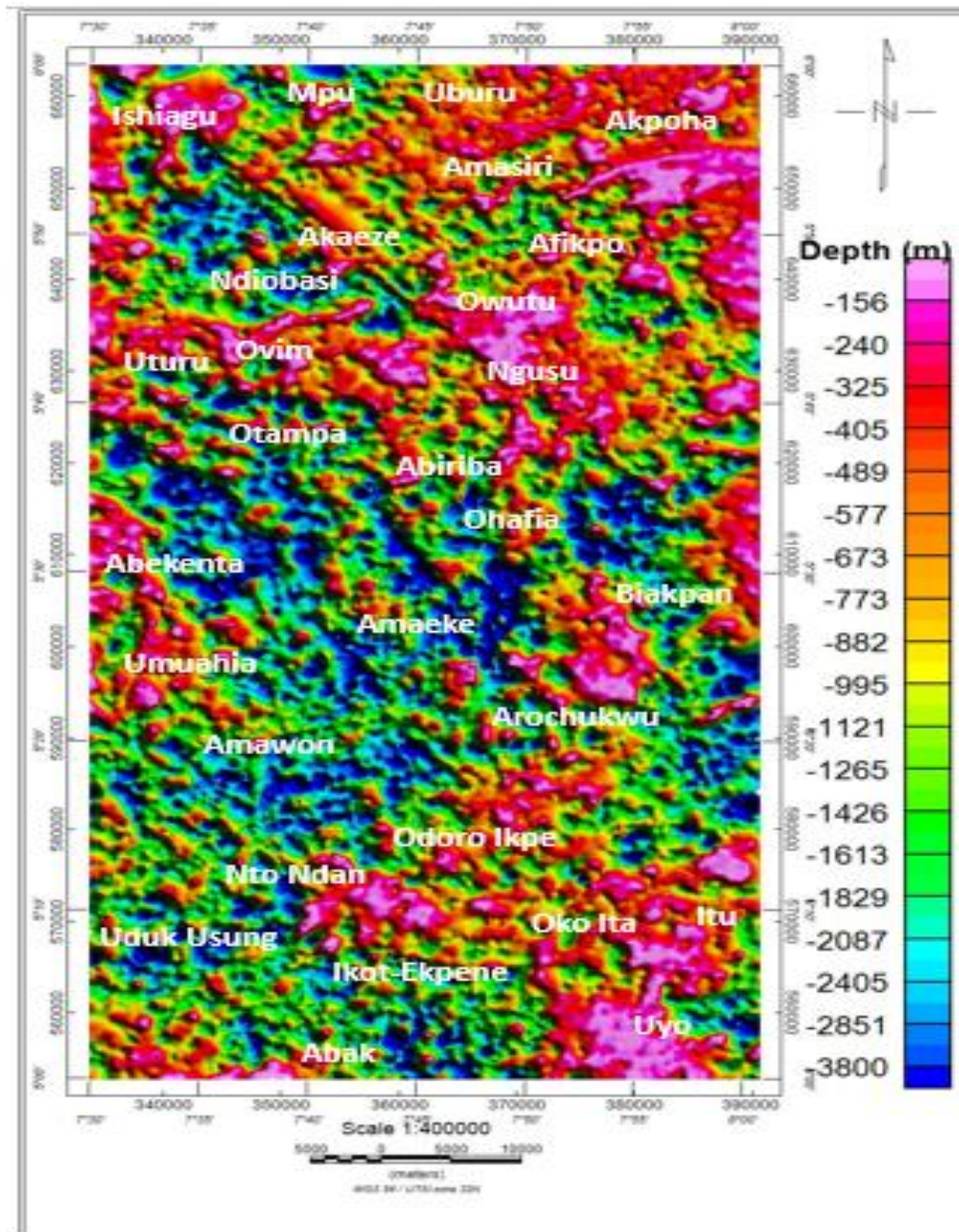


Figure 8: Source Parameter Imaging (SPI) Map of the Study Area

3.2 Discussion

The total magnetic intensity shows the effects of the underlying basement as well as effects of intrusives within the study area. The area is characterized by high, intermediate, and low amplitude anomalies with magnetic intensities range of 7736 nT minimum to above 7962 nT, but dominated by high to intermediate intensities at the northern part of the study area and moderate to low at the southern part. The TMI map (Figure 3) shows the highest susceptibility values (≥ 7892 nT corresponding to the area with pink and red colour) at the northern and eastern parts of the study area. The alignment of the magnetic high occurs along the strike of the present Afikpo Basin and coincides with the igneous rocks and intrusives of Uburu, Uturu, Ishiagu, Akaeze and Afikpo. The magnetic high observed at east of Afikpo and east of Arochukwu areas corresponds to the southeastern Basement Complex of Nigeria. The intermediate susceptibility values (7787 – 7892 nT,

corresponding to the area with green to yellow colours) represent the lower – middle Cretaceous sedimentary rocks which host igneous intrusives and also occupy the greater part of the central and southwest of the study area. The least susceptibility values (< 7787 nT corresponding to the area with blue colour) occurring at the central and southeast of the study area, represent sedimentary deposits of the uppermost Cretaceous – Tertiary age and Alluvium. The zones of low magnetic intensity are defined as response from deep seated magnetic sources with thick sediments/ sedimentary rocks cover, intermediate are interpreted as response from highly consolidated ferruginized sediments or near surface magnetic sources, and high intensities are response from shallow or surface magnetic sources of possible basement rocks/intrusives and intense ferruginized sediments.

The TMI map shows that the long wavelength and low frequency body trending NE-SW at the northern part indicate that the depth to magnetic basement in these areas is relatively high. Magnetic crest and trough is observed at the central part of the study area and is interpreted as a major fault zone within the area. Four regional fault zones were defined in the study area including the Abakaliki Anticlinorium- Afikpo Syncline fault that yielded the Afikpo Basin (AA-AB in Figure 9), Central fault system (CF in Figure 9), Umuahia-Amawon fault system (UH-AM) and Abak-Ikot Ekpene fault (AB-EK). Short wavelength or high frequency structures are observed to spread around the study area and they are interpreted as intrusives.

The analytic signal was computed to enhance the edge of the shallow magnetic source (Ansari and Alamdar, 2011). This was done in order to identify mineralized and intruded zones within the study area. The bodies at the east of the area (yellow polygon in Figure 10) are defined to be responses from granite, migmatite gneiss and diorite rocks associated with the Oban Massif. The high magnetic response observed at Ishiagu results from diorite intrusions and hydrothermally formed lead-zinc mineralization associated with the Southern Benue Trough. Intrusives within the Afikpo were defined as prominent around Arochukwu, Afikpo, Biakpan, Ngusu, Ohafia, Owutu, Uturu, Ovum, Umuahia, Abekenta, Uyo, Nto Ndan and Otampa areas. These intrusives were interpreted as diorite sills and dykes associated with the Afikpo Basin. They were installed during the formation of the Basin by the Santonian Orogeny that lead to the formation of the Abakaliki Anticlinorium and Afikpo Syncline. Less intrusives are observed around Uburu and Mpu (Southern Benue Trough) and Abak, Amawon, Amaeke, Akaeze, Oko Ita, Odoro Ikpe, Uduk Usung and south of Arochukwu. The moderate to low magnetism observed at Uburu, Akpoha, Amasiri, Owutu, Ngusu, Akaeze, Amaeke, Arochukwu, Umuahia and Odoro Ikpe resulted from the alteration rocks by thermal action that produced the intrusives. This made most of the country rocks indurated and hence quarried by host communities for construction. The moderate susceptibility is majorly due to ferruginization.

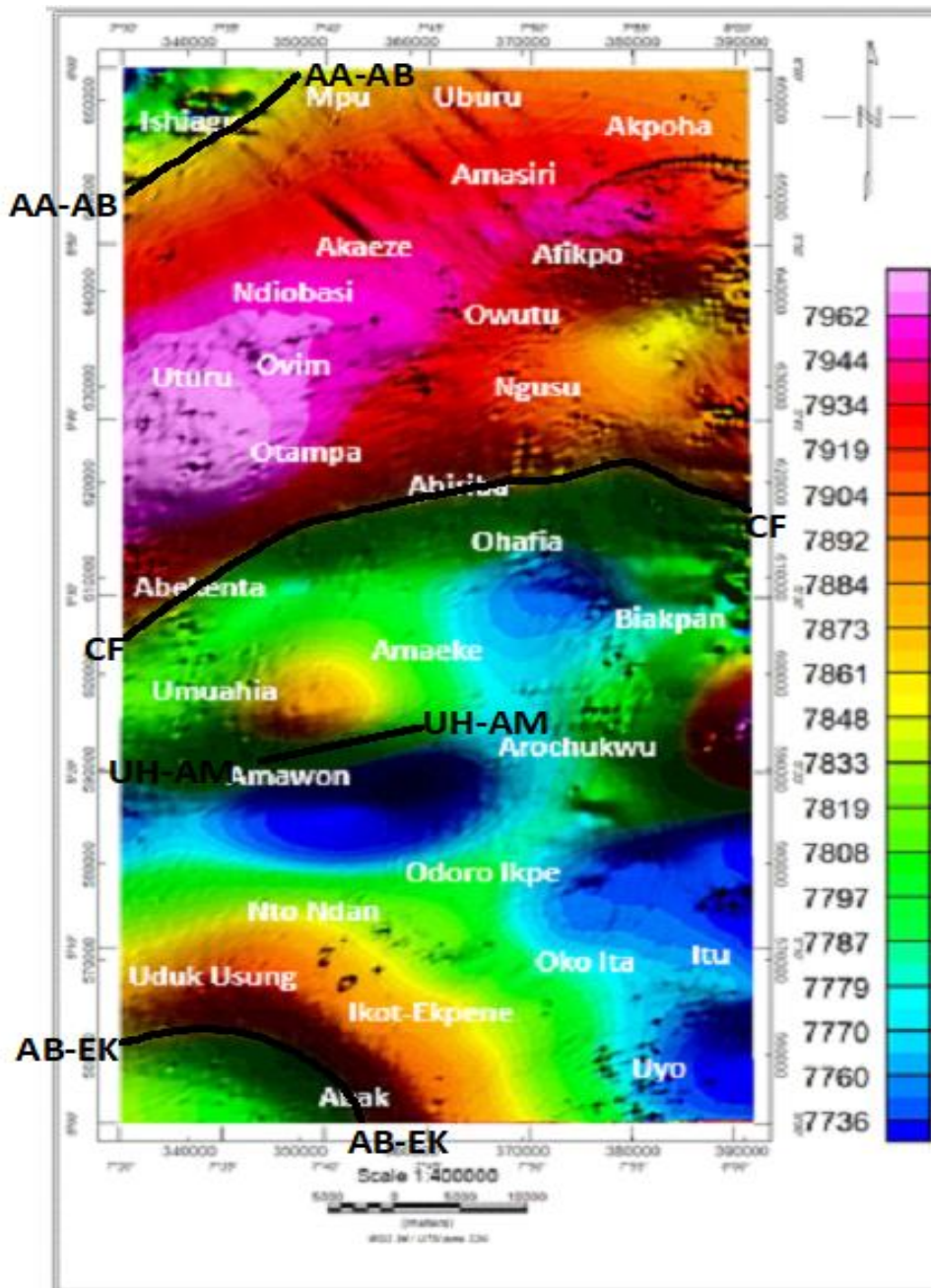


Figure 9: Total Magnetic intensity Map of the Study Area Showing Regional Fault

The FVD map (Figure 6) shows inferred faults, fractures, folds, contacts and to some extent the shape of some lithologic contacts which indicate structural features. Fault and fracture system were observed between Uburu and Akpoha, Amasiri area (blue polygon in Figure 11); these were interpreted to have formed during the shearing and faulting of the Southern Benue Trough that yielded the Afikpo Basin during the Santonian Age. The longest of the faults stretches to about 3.4 km within the study area, trending NE-SW, hence resulting from NW-SE compression of the Basin. A sill (yellow polygon in Figure 11) is observed to stretch from Afikpo through Amasiri to Akpoha and seems to be continuous towards Ugep. The defined diorite sills correspond to that early defined by Ani et al (2017) where it was defined to be about 16.4 km in length and 1.3 km in width. Within the study area, the sill is about 1.9 km (red polygon in Figure 11). The intrusives within Ishiagu and Uyo are greatly enhanced (green polygon in Figure 11) and show a major NE-SW trend. The regional fault UH-AM was also better enhanced in the FVD map.

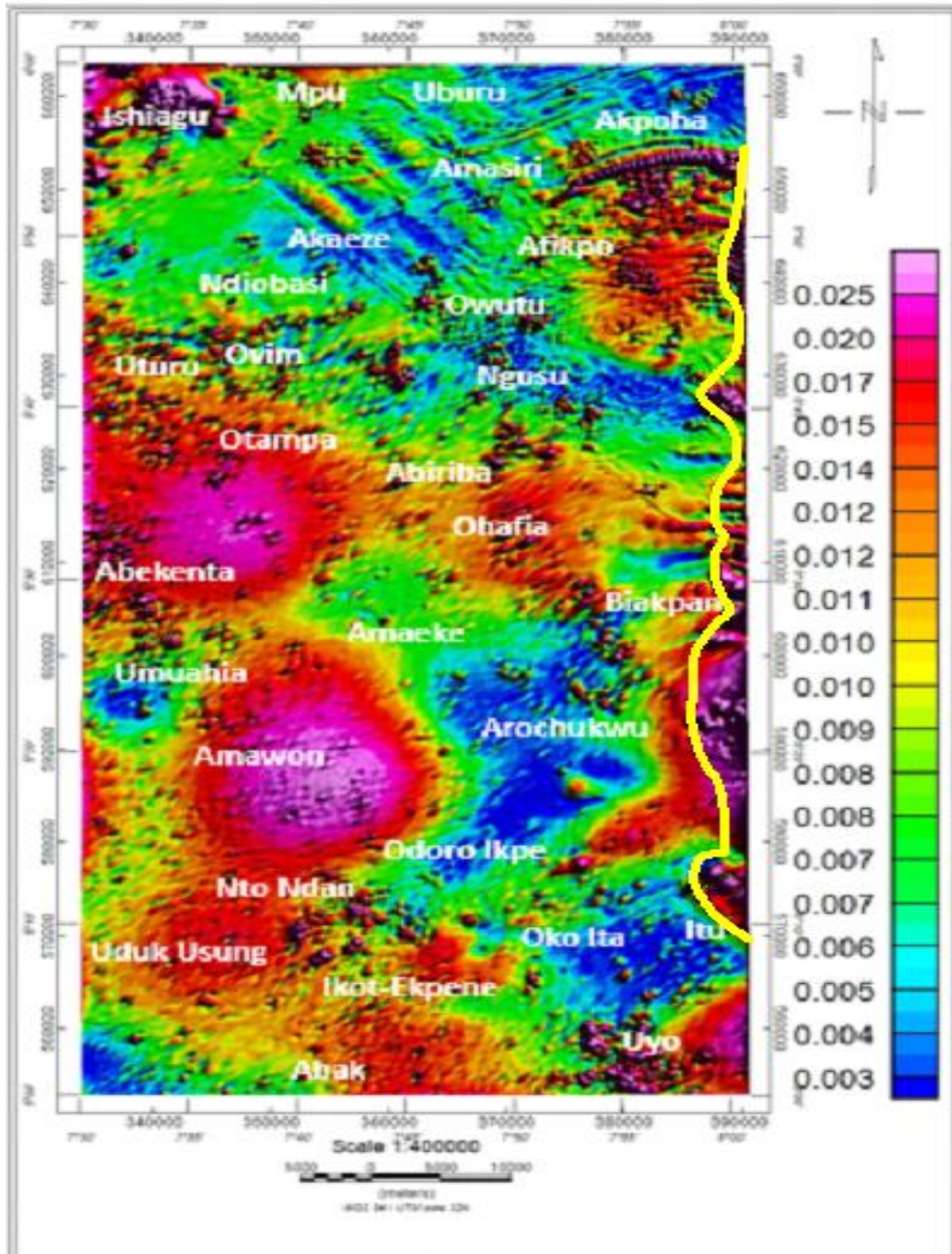


Figure 10: Analytic Signal Map of the Study Area

In the eastern part of Afikpo, Itu and Biakpan, the basement rocks show intense faulting and folding. This deformation and folding was as a result of the pronounced deformation and remobilization that occurred during the Pan-African orogeny about 650-450 million years ago (Odeyemi, 1981).

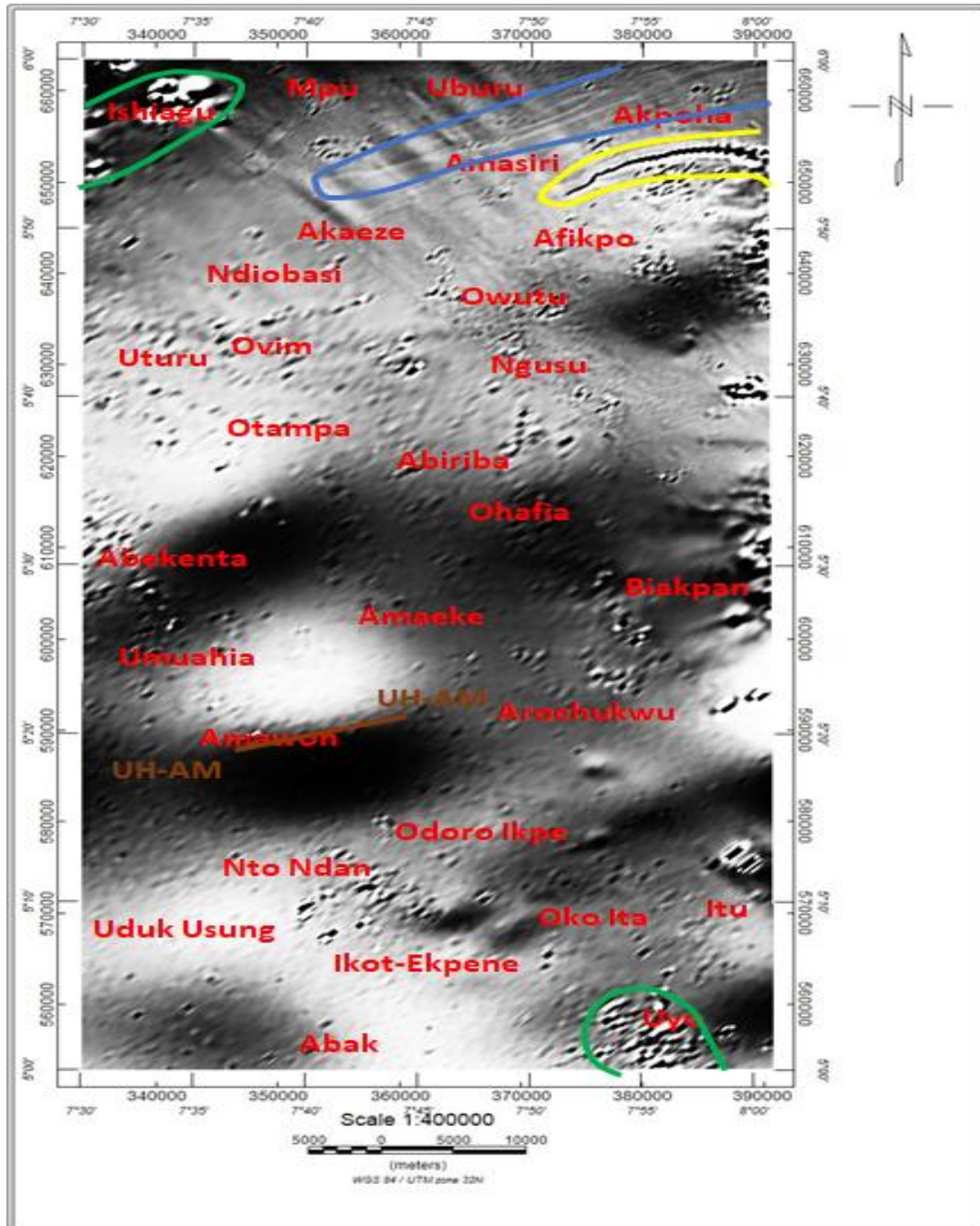


Figure 11: First Vertical Derivative (FVD) Map of the Study Area Showing Fault, Sill/Dyke

Lineament map (Figure 7) provides an insight of the geological structural control and lithologic deformations in the study area. Lineaments result from faults, joints, folds, contacts or other geological reasons, found in igneous, sedimentary and metamorphic rocks (Megwara and Udensi 2014). The lineaments (faults) are marked in black ticks while dykes and sills are marked in arched curves. The orientation and length of the lineament extracted from the Vectorization lineament map (Figure 7) were displayed in a rose diagram to analyze the spatial distribution of lineaments. The rose diagram (Figure 7) shows that the structures within the study area trend majorly NE-SW and EW with minor NW-SE, N-S directions.

From the extracted lineaments, the structures within Afikpo Basin (representing the largest) trend in the NE-SW direction with minority striking in the NS and NW-SE direction. The defined trends are in agreement with earlier work by Zarboski (1998) and Nwajide (2013) on the Benue Trough and Afikpo Basin respectively. Five major dykes/sills were observed in the study area with the longest running from Afikpo to Akpoha (yellow polygon in Figure 11), the second is observed at Itu (green polygon in Figure 12) and the third at Ishiagu (blue polygon in Figure 12).

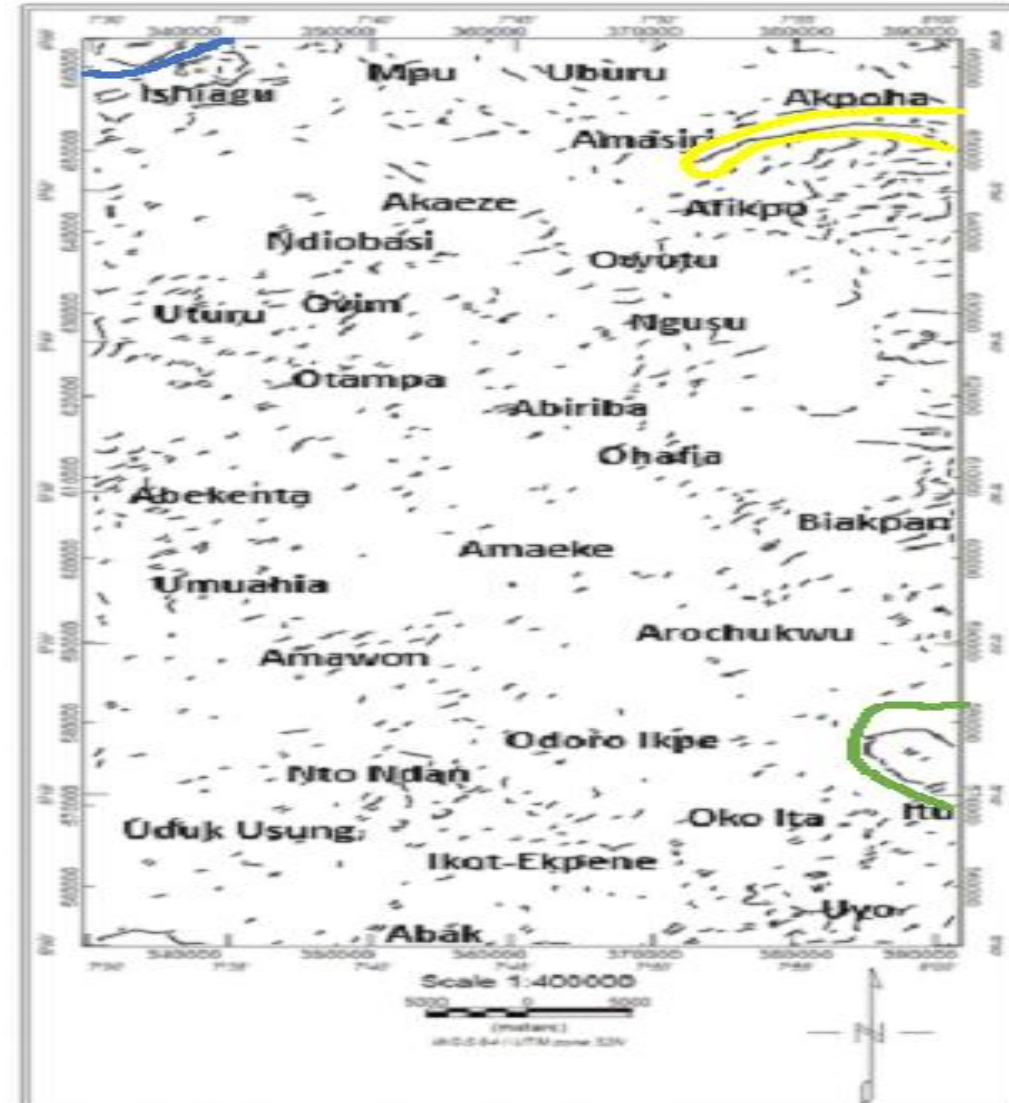


Figure 12: Lineament Map and Rose Diagram of the Study Area Showing defined Sills/Dyke

The intensity of deformation was evaluated using the lineament density of the study area (Figure 13). Areas of intense deformation include east of Afikpo, east of Biakpan, Itu, Uyo, Nto Ndan, Abekenta, Uturu, Otampa, Ovim, Owutu, Ngusu, Ishiagu and Mpu. Moderate deformation is observed at Amasiri, Akaeze, Abiriba, Ohafia, Udjuk Usung, Abak, Odofo Ikpe. Low deformed areas include Arochukwu, Uburu, Amaeka, Amawon and Oko Ita. Structural complexity is important to formation of traps for hydrocarbon accumulation. Highly deformed area could lead to the destruction of stratigraphic traps and enhance the occurrence of structural traps but due to its intensity it could yield leakage of traps due to micro faults or total destruction of structural trap, hence, moderately deformed area host better structural traps.

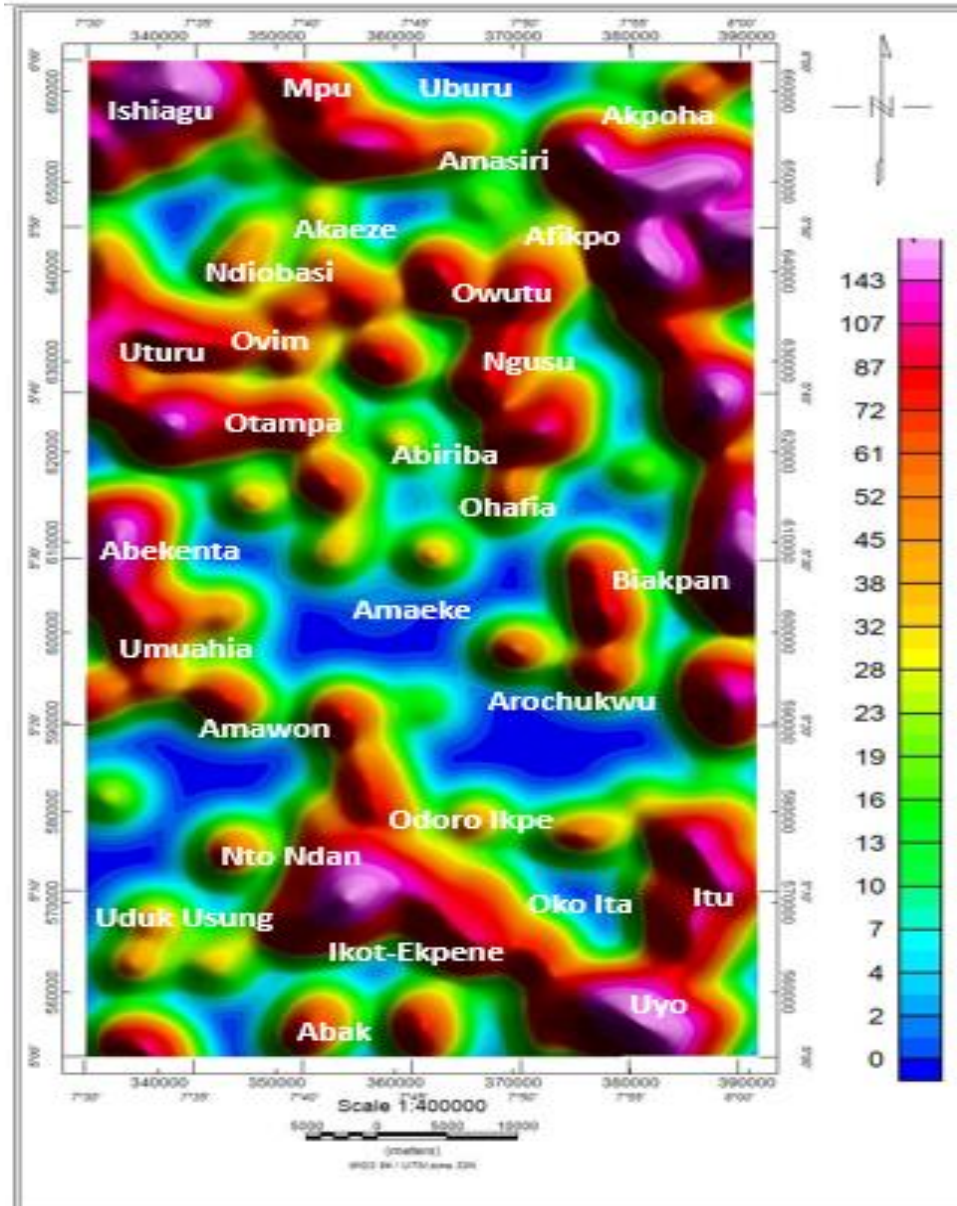


Figure 13: Lineament Density Map of the Study Area

The SPI map (Figure 8) shows the depth estimate to the basement surface (i.e. top of the sediment/basement interface). The negatives in the numbers on the legend signify depth to the buried magnetic sources. Uburu, Akpoha, Ishiagu, Uyo, west of Umuahia, Abakenta, Uturu, Ovim, Odoro Ikpa, east of Afikpo and east of Biakpan show depth to basement less than 500 m. Moderate depth to basement with range of 500 m – 1.9 km is observed at Afikpo, Amasiri, Umuahia, Abiriba, south of Abak, east of Ngusu, Oko Ita and Itu while depth ≥ 1.9 km is observed at Otampa, Amaeke, Akaeze, Ndiobasi, south of Ohafia, Amawon, Uduk Usung, Nto Ndan and Ikot Ekpene.

The SPI map indicates variable depth to basement rocks which is synonymous to thickness of overburden sediment and this has a very important significance as regards to the hydrocarbon generation potential (Nwosu, 2014). Wright et al (1985) showed that the minimum thickness of sediment required to achieve the threshold temperature of 115°C for the commencement of oil formation from organic remains would be 2.3 km deep when all other conditions for hydrocarbon accumulation are favourable and the average temperature gradient of 1°C for 30 m obtainable in oil rich Niger Delta is applicable. Based on this fact colour ramp filter was applied to highlight areas with sediment thickness ≥ 2.3 km (Figure 14).

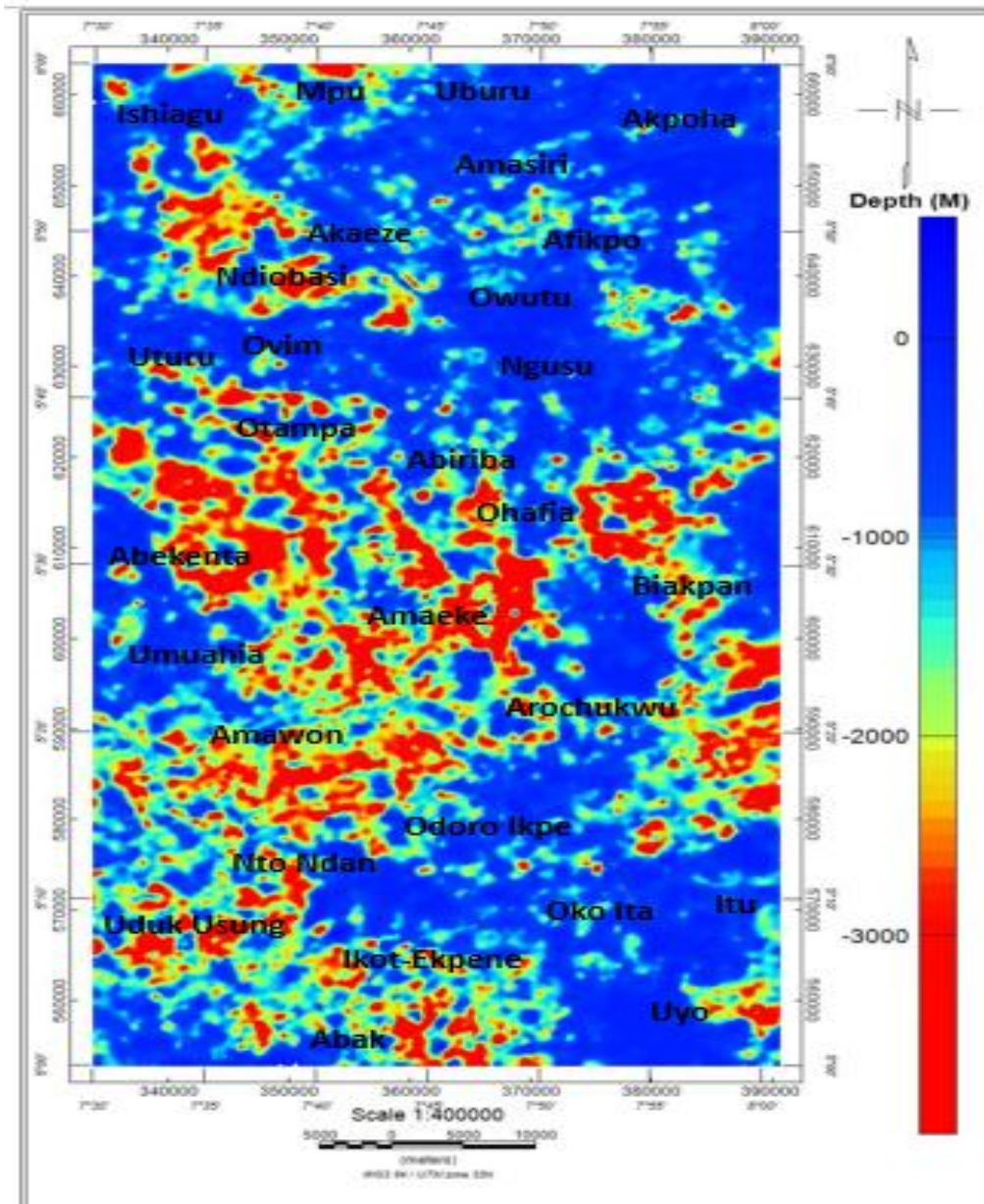


Figure 14: Colour Ramp Source Parameter Imaging Map of the Study Area

Areas with thick sedimentary cover include Ndiobasi, northwest of Akaeze, Ikot Ekpene, east of Uyo, Uduk Usung, Nto Ndan, Amawon, Abekenta, Amaeke, south of Ohafia and Otampa. The sediment thickness within these areas is suitable for the commencement of hydrocarbon generation from organic rich sediments. For better interpretation and integration of structural and depth analysis six profiles were taken on the FVD, analytic signal and SPI map (Figure 15). Figures 16 – 21 show modeled depths for the profiles.

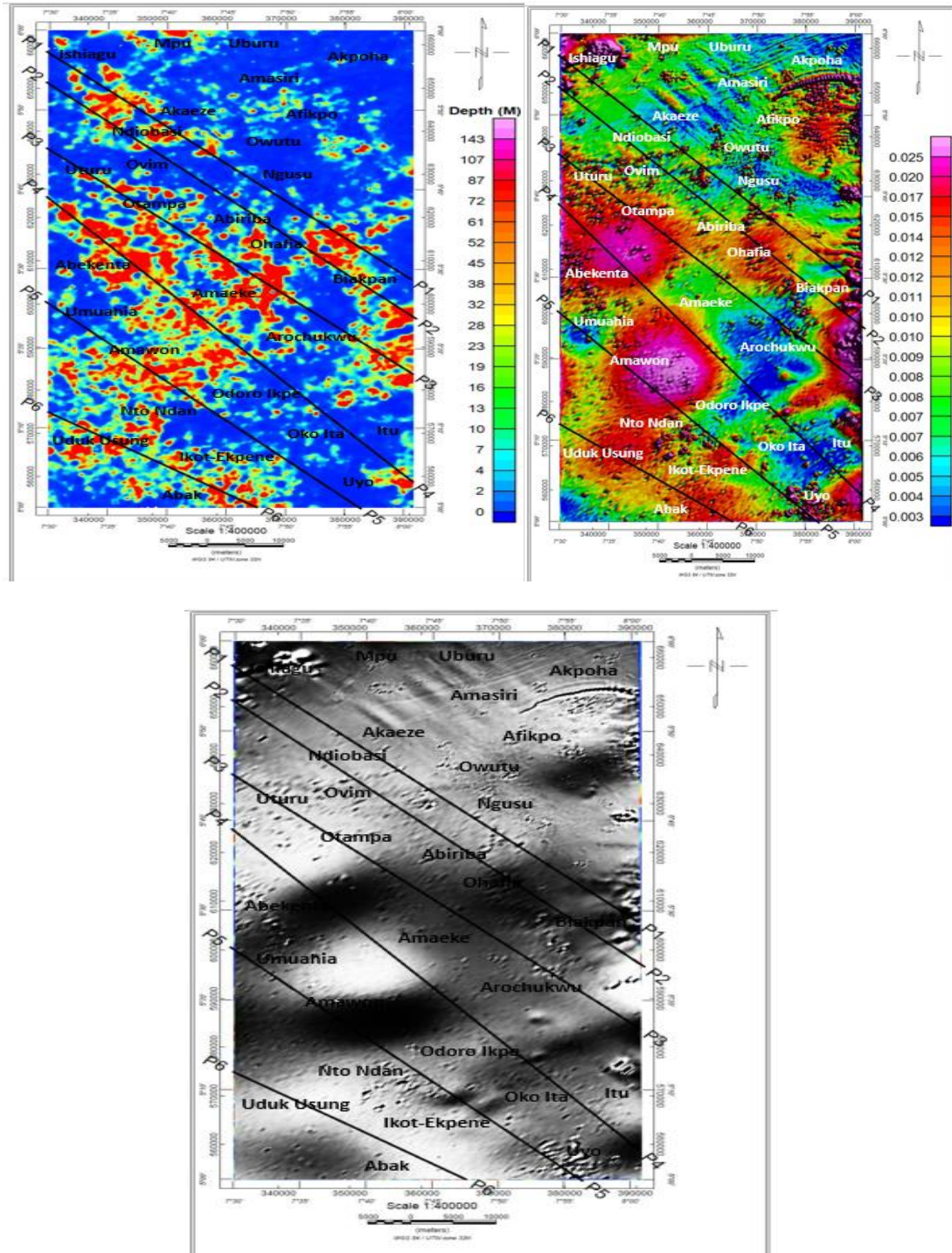


Figure 15: Profile along the SPI, Analytic Signal and FVD Maps

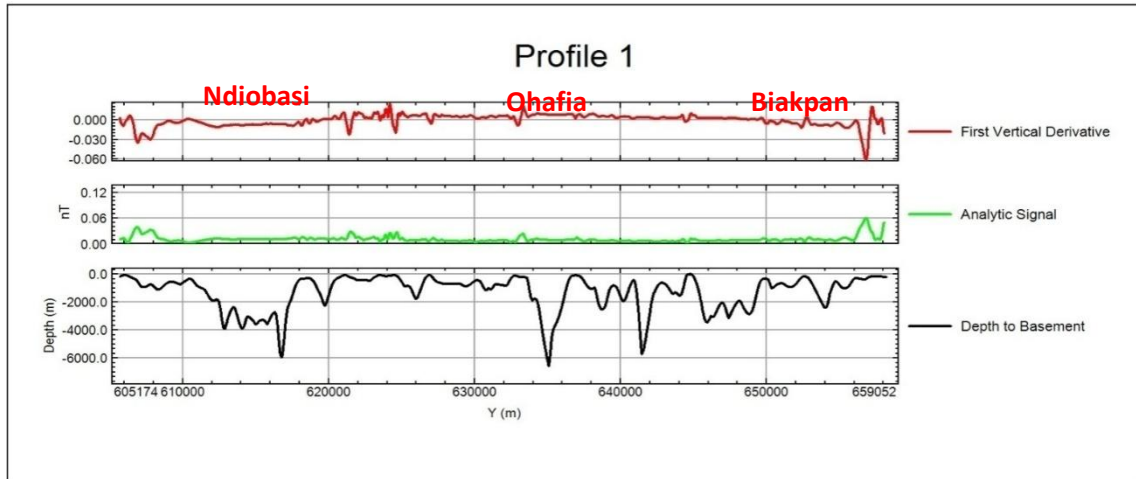


Figure 16: Modeled Depths for Profile 1

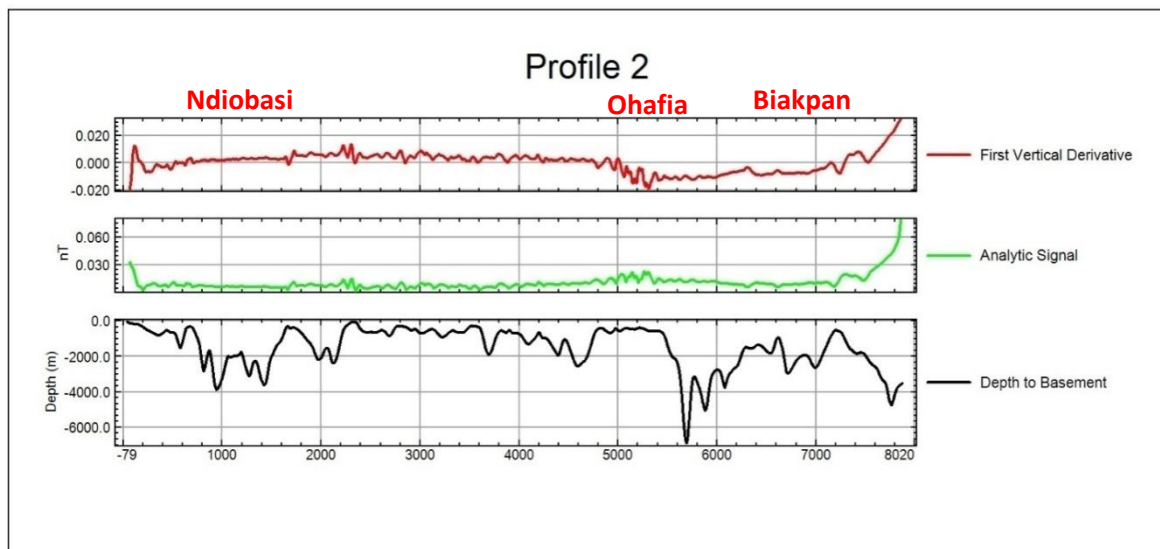


Figure 17: Modeled Depths for Profile 2

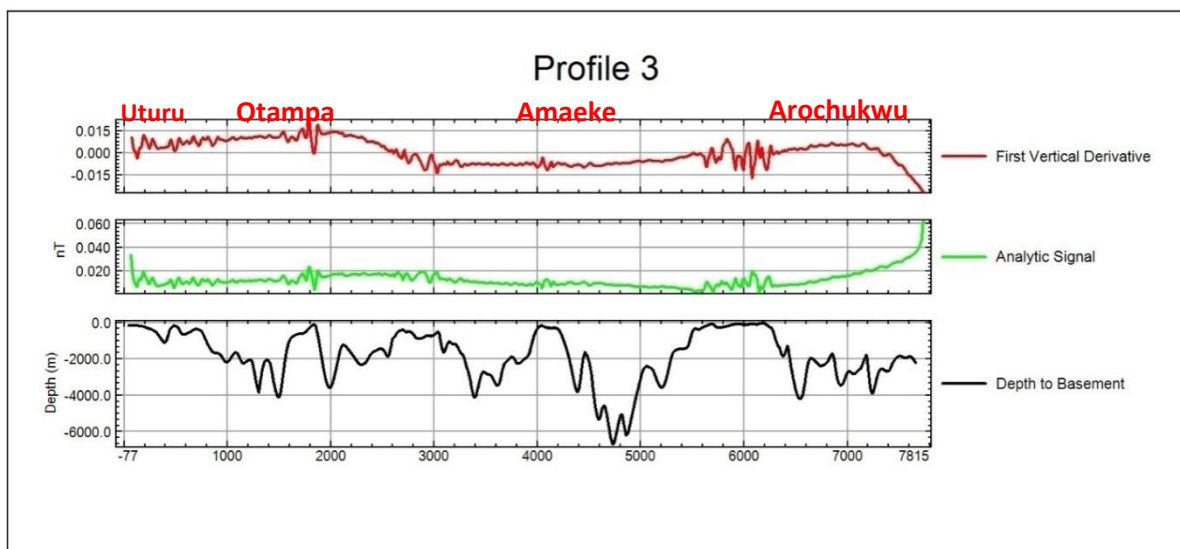


Figure 18: Modeled Depths for Profile 3

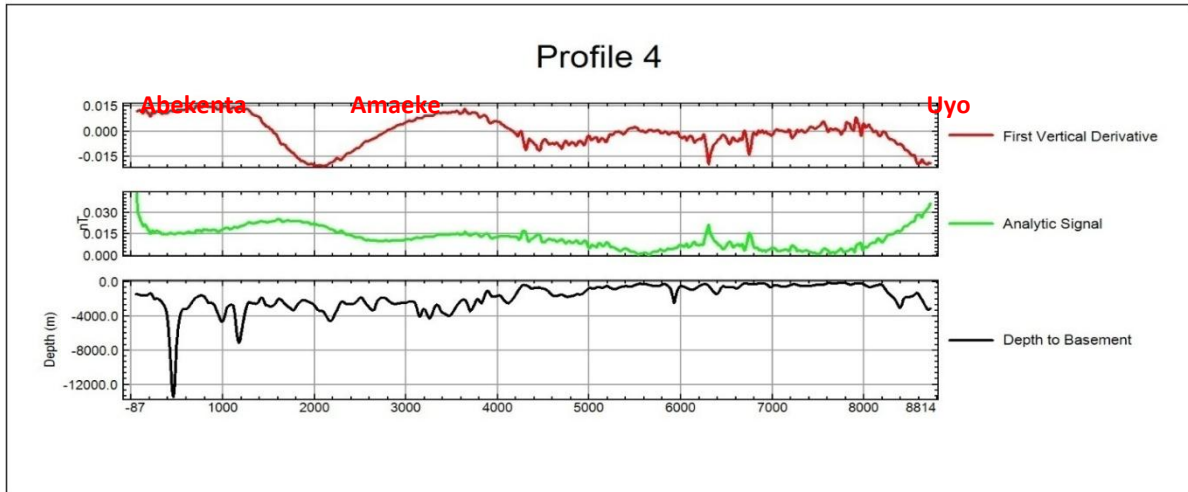


Figure 19: Modeled Depths for Profile 4

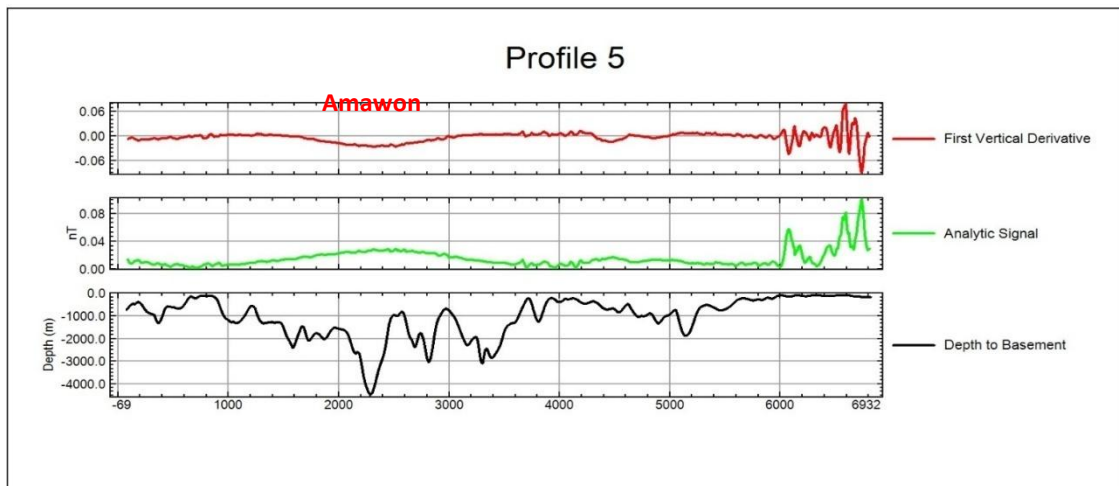


Figure 20: Modeled Depths for Profile 5

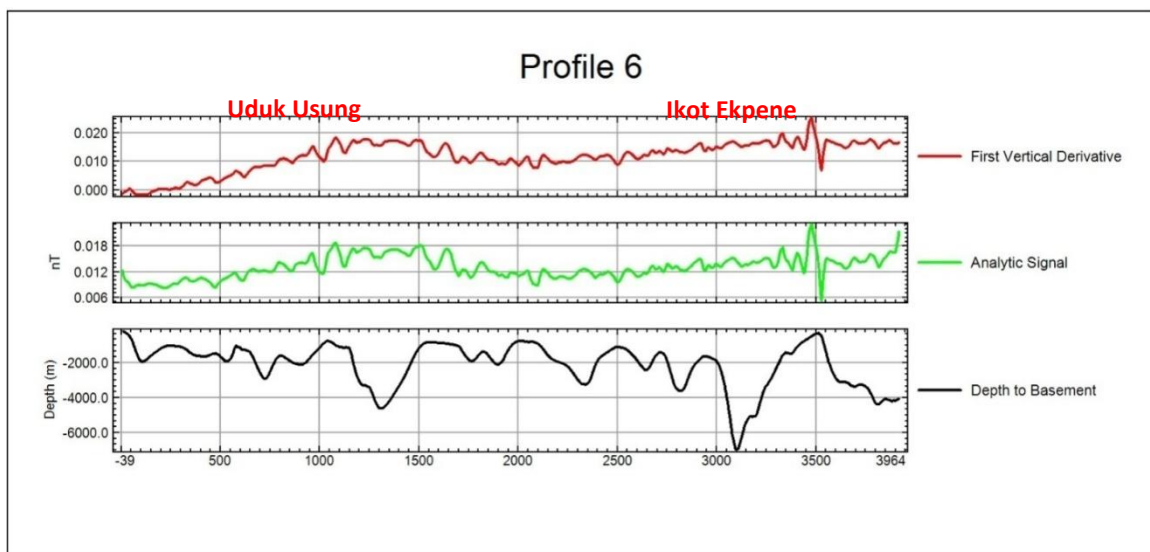


Figure 21: Modeled Depths for Profile 6

The modeled depths for Profile 1 (Figure 16) show a sedimentary thickness range of 0.1 – 5.8 km around Ndiobasi, 2.5 – 5.5 km around Ohafia and 0.1 – 3.4 km at Biakpan. Ndiobasi area shows low deformation while Ohafia and Biakpan areas show moderate deformation. Along Profile 2 (Figure 17) south of

Ndiobasi has sediment thickness range of 2.3 – 3.8 km, east of Ohafia has 0.1 – 6.6 km and Biakpan has 0.5 – 4.7 km. Ndiobasi and Ohafia areas show moderate deformation and Biakpan shows high deformation. Profile 3 (Figure 18) shows Otampa with 0.1 – 4 km, Amaeke has sediment thickness range of 2.2 – 6.7 km, while Arochukwu area shows thickness of 1.8 – 4.2 km; all the three areas show moderate deformation. Abekenta has sediment thickness range of 2.5 – 12 km, Amaeke has 2.4 – 4.4 km while Uyo has 0.3 – 2.8 km along Profile 4 (Figure 19), and all the three areas also show moderate deformation. Along Profile 5 (Figure 20) Amawon has sediment thickness of 0.8 – 4.4 km and the sediment reflects low deformation. On Profile 6 (Figure 21) Uduk Usung has a sedimentary thickness of 0.7 – 4.5 km while Ikot Ekpene has 1.5 – 6.9 km, and both areas show high deformation within the sediments. Since the depths within these areas are greater than 2.3 km they are selected as areas for future prospect for hydrocarbon.

IV. Conclusion

The hydrocarbon potential of Afikpo Basin was evaluated by defining the structural complexity and sediment thickness within the basin. This was achieved by the processing and filtering of aeromagnetic data using trend analysis, first vertical derivative, analytic signal and source parameter imaging.

The structures within the basin trends majorly in the NE-SW direction with minor NW-SE and NS trends. Lineament density analysis showed that sediments at the east of Afikpo, east of Biakpan, Itu, Uyo, Nto Ndan, Abekenta, Uturu, Otampa, Ovim, Owutu, Ngusu, Ishiagu and Mpu underwent intense deformation. Amasiri, Akaeze, Abiriba, Ohafia, Uduk Usung, Abak, Odoro Ikpe sediments underwent moderate deformation while Arochukwu, Uburu, Amaeke, Amawon and Oko Ita sediments experience the least level of deformation.

Four regional fault zones were defined and include Abakaliki Anticlinorium- Afikpo Syncline fault that yielded the Afikpo Basin, Central fault system, Umuahia-Amawon fault system and Abak-Ikot Ekpene fault.

The depth analysis shows that Ndiobasi area has an average sedimentary thickness of 4.5 km, Ohafia has an average of 2.6 km, Biakpan has an average of 2.1 km, Otampa has an average of 2.0 km, Amaeke has an average of 3.9 km, Arochukwu area has an average of 3.0 km, Uyo has an average of 1.5 km, Uduk Usung has an averages of 2.6 km and Ikot Ekpene has an average of 4.2 km. Ndiobasi, Ohafia, Biakpan, Amaeke, Arochukwu, Uduk Usung and Ikot Ekpene were recommended for further studies for hydrocarbon prospecting on the bases of their sediment structural complexity and sediment thickness.

Reference

- [1]. Ani, C.C., Iduma U., Adelekan, A., and Chukwu. A. (2017). Structural Analysis of Afikpo Synclinorium Using First Vertical Derivative and Horizontal Gradient, South-Eastern Nigeria. Nigerian Mining and Geoscience Society, Abuja 2017. Pp 43
- [2]. Ansari, A. H., and Alamdar, K. (2011). A New Edge Detection Method Based On The Analytic Signal Of Tilt Angle (ASTA) For Magnetic And Gravity Anomalies. Iranian Journal of Science and Technology A2, Pp. 81 – 88
- [3]. Anyanwu, G. and Mamah, L. (2013). Structural interpretation of Abakaliki-Ugep; using Airborne magnetic and Landsat thematic mapper (TM) data. Journal of natural sciences research, Vol.3, No.13, pp.137-146.
- [4]. Benkheilil J (1982). Benue Trough and Benue Chain. Geological Magazine 119: 155 – 168.
- [5]. Benkheilil, J. (1989). The Evolution of the Cretaceous Benue Trough, Nigeria. Journal of African Earth Sciences, 8: 251 – 282.
- [6]. Benkheilil, Guirid, M., Pondard, J.F. and Saugy, L., (1989). The Bornu-Benue Trough, the Niger Delta and its offshore: Tectono-Sedimentary Reconstruction During the Cretaceous and Tertiary from Geophysical Data and Geology. In: Kogbe, C.A. (Ed.): Geology of Nigeria. Rock View (Nig.) Ltd., pp. 277-309.
- [7]. Burke, K.C., Desavaugie, T.F.J., and Whiteman, A.J. (1972). Geology History of the Benue Valley and Adjacent Areas. In: Desavaugie, T.F.J. and Whiteman, A.J. (eds.) African Geology. University of Ibadan Press, Nigeria.
- [8]. Davis, J.C., (1973). Statistic and Data Analysis in Geology. Wiley International Edition, Pp. 322 – 327.
- [9]. Fairhead, J.D. (1988). Mesozoic Plate Tectonics Reconstructions of the Central South Atlantic Ocean: the Role of the West and Central African Rift System. Journal of Tectonophysics 187: 231 -249.
- [10]. Genik, G.J. (1993). Petroleum Geology of Cretaceous – Tertiary Rift Basins in Niger, Chad and Central African Republic. American Association of Petroleum Geologists Bulletin 77: 1405 - 1434.
- [11]. Hoque, M. (1977). Petrographic Differentiation of Tectonically Controlled Cretaceous Sedimentary Cycles, Southeastern, Nigeria. Journal of Sedimentary Geology 17: 235- 345.
- [12]. Luo, Y., Wang, M., Luo, F. and Tian, S. (2011). Direct Analytic Signal Interpretation Of Potential Field Data Using 2-D Hilbert Transform. Chinese Journal of Geophysics Vol.54, No.4, pp. 551 – 559
- [13]. Megwara, J.U. and Udensi, E.E., (2014). Structural analysis using aeromagnetic data: case study of parts of Southern Bida basin, Nigeria and the surrounding basement rocks. Earth science research, Vol.3, No.2, pp.27-36.
- [14]. Murat, R.C. (1972). Stratigraphy and Paleogeography of the Cretaceous and Lower Tertiary in Southern Nigeria In: T. F. J. Dessauvagie and A. J. Whiteman (Eds). African Geology. University of Ibadan, Nigeria, 201-266.
- [15]. Nabighian, M. N. (1972). The analytical signal of two-dimensional magnetic bodies with polygonal cross-section: its properties and use for automated anomaly interpretation Geophysics, 37(3):507– 517.
- [16]. Nwajide, C.S. (2006). Outcrop analogies as a learning facility for subsurface practitioners: the value of geology field trips. Petroleum training journal, v.3, p.58-68.
- [17]. Nwajide, C. S. (2013). Geology of Nigeria's Sedimentary Basins. CSS bookshops limited.. Pp 290
- [18]. Nwosu, O.B. (2014). Determination of Magnetic Basement Depth Over Parts Of Middle Benue Trough By Source Parameter Imaging (SPI) Technique Using HRAM International Journal of Scientific and Technology Research 3, 262-271.
- [19]. Odeyemi, I.B. (1988). Lithstratigraphy and Structural Relationship of the Upper Precambrian Metasediments in Igarra south western Nigeria in Precambrian Geology of Nigeria, Geological Survey of Nigeria, Kaduna South, pp.111-125.
- [20]. Onuba, L.N., Anudu, G.K., Chiaghanam, O.I., and Anakwuba E.K. (2013). Evaluation of Aeromagnetic Anomalies over Okigwe Area, Southeastern Nigeria. Journal of Environmental and Earth Sciences, Vol. 3, No.5, Pp. 498-507.

- [21]. Onwuemesi A.G. (1995). Interpretation of magnetic anomalies from the Anambra Basin of southeastern Nigeria. Ph.D thesis, Nnamdi Azikiwe University, Awka, Nigeria.
- [22]. Onwuemesi, A.G. (1997). One-Dimensional Spectral Analysis of Aeromagnetic Anomalies and Curie Depth Isotherm in the Anambra Basin Of Nigeria. *J. Geodyn.*, Vol. 23, No.2, Pp. 95 - 107.
- [23]. Petre, S. and Randolph, L.M. (2015). *Spectral Analysis of Signals*. Prentice Hall. 0-13-113956-8
- [24]. Reyment, R. A. (1965). *Aspects of the Geology of Nigeria*. Ibadan University Press. 124- 135.
- [25]. Siddorn, J.P. and Halls, H.C. (2002). Variation in plagioclase clouding intensity in Matachewan dykes: evidence for the exhumation history of the northern margin of the Sudbury igneous complex. *Can. J. Earth Sci.* 39, 933-942
- [26]. Simpson, A. (1954). The Nigerian Coal Field, Geology of Parts of Onitsha, Owerri and Benue Provinces. *Bull. Geol. Surv. Nig.* 24, 1 – 31.
- [27]. Smith, R. S., Thurston, J. B., Dai Ting-Fan and Ian, N. M. (1998). iSPITM- the improved source parameter imaging method. *Geophysical prospecting*, 46, 141-151.
- [28]. Thurston, J. B., Smith, R.S., and Guillon, J.C. (2002). A multimodel method for depth estimation from magnetic data: *Geophysics*, 67, 555–561
- [29]. Thurston, J., Guillon, J.C., and R. Smith, R. (1999). Model-independent depth estimation with the SPITM method: 69th Annual International Meeting, SEG, Expanded Abstracts, 403–406
- [30]. Thurston, J.B., Smith, R.S., (1997). Automatic Conversion of Magnetic Data to Depth, Dip and Susceptibility Contrast Using SPI Method. *Geophysics*, Vol. 62, No.3, Pp. 807-813.
- [31]. Ugbor, D.O., and Okeke, F.N. (2010). Geophysical investigation in the lower Benue Trough of Nigeria, using gravity method. *Int. J. Phys. Sci.* 5(11):1757–1769.
- [32]. Ugwu, G.Z., and Ezema, P.O. (2012). Forward and inverse modelling of aeromagnetic anomalies over Abakaliki and Nkalagu areas of the Lower Benue Trough, Nigeria. *Int. Res. J. Geol. Min.* 2(8):222-229.
- [33]. Ugwu, G.Z., Ezema, P.O., and Ezech C.C. (2013). Interpretation of aeromagnetic data over Okigwe and Afikpo areas of lower Benue Trough, Nigeria. *Int. Res. J. Geol. Mining.* 3(1):1–8
- [34]. Uzuakpunwa A.B. (1974). The Abakaliki pyroclastics-eastern Nigeria: New age and tectonic implications. *Geol. Mag.* 111:761-769.
- [35]. Wright, J.B., Hastings, D.A., Jones, W.B., and Williams, H.R. (1985) *Geology and Mineral Resources of West Africa*. George Allen and Unwin, London.
- [36]. Zaborski, P. M. (1998). A review of the Cretaceous System in Nigeria. *Africa Geoscience Review* 5, pp. 385 – 483.

IOSR Journal of Applied Geology and Geophysics (IOSR-JAGG) is UGC approved Journal with Sl. No. 5021, Journal no. 49115.

Ibe Stephen and Uche Iduma, "Hydrocarbon Potential of Nigeria's Inland Basin: Case Study of Afikpo Basin." *IOSR Journal of Applied Geology and Geophysics (IOSR-JAGG)* 6.4 (2018): 01-24.